J Mater Sci (2007) 42:5835–5844
DOI 10.1007/s10853-006-1390-z

Evaluating environmental stress cracking thresholds by contact angle measurements

Peter J. Walsh · Alan J. Lesser

Received: 23 September 2004 / Accepted: 13 January 2006 / Published online: 23 May 2007

Abstract This work probes a hypothesis for predicting a critical stress associated with of environmental stress cracking (ESC). The hypothesis is based on a thermodynamic criterion for localized swelling induced by stress on the polymer. The surface-active liquids chosen for study are oleic acid and dibutyl phthalate and the polymer is polycarbonate (PC). An experimental technique involving contact angle measurements of a sessile drop as a function of stress is used to probe the hypothesis. A new method for measuring contact angle using refraction is also introduced. No significant change in contact angle as function of stress is observed in either system, though the kinetics of craze initiation and inelastic strain at craze initiation do show a shift in response to stress at levels similar to those predicted by the hypothesis.

Introduction

A glassy polymer exposed to certain surface-active agents while under moderate stress may develop crazes and subsequently fail prematurely in an apparently brittle manner, a phenomenon commonly referred to as environmental stress cracking or crazing (ESC). Close examination of the crazed regions of the polymer show that highly oriented drawn or fibrillated regions evolve locally, that over time, develop into cracks and subsequently cause brittle failure. Crazes are typically between 100–1000 nm in thickness and the elongated material within the craze may be fibrillar [1] or simply regions of highly drawn material [2]. It is generally believed that crazes initiate because a surface-active agent locally plasticizes the polymer thereby causing a local reduction in glass transition temperature (T_g) leading to premature yielding and plastic flow.

A hypothetical crazing mechanism proposed by Gent, and further investigated by Mai and Yee [3–6] states that the uptake of the surface-active liquid into the polymer, and resulting plasticization, is stress activated. Specifically, stress induced swelling is proposed to occur because the dilatational component of the applied tensile stress increases the equilibrium volume fraction of surface-active liquid in the polymer. It is further proposed that the liquid molecules are generally small enough that the volume they displace can be considered equivalent to added free volume in the glassy polymer. At some critical hydrostatic stress the free volume increases enough that the polymer transitions from a glassy to a rubbery state. Gent suggests that asperities at the polymer surface lead to local stress concentrations thereby causing locally high hydrostatic tension, which become preferential sites for localized swelling and subsequent craze development.

The Gent hypothesis qualitatively accounts for some commonly observed characteristics of ESC: (i) Hydrostatic compression tends to prevent the onset of crazing. (ii) The critical crazing stress is temperature dependent and decreases as T_g is approached. (iii) The tensile stress at which crazing occurs when a surface-active liquid is present is much reduced, and the liquids tend to have solubility parameters similar to, but less than the polymer, such that they are not fully

P. J. Walsh (✉) · A. J. Lesser
Department of Polymer Science and Engineering,
University of Massachusetts, Amherst, MA 01003, USA
e-mail: pjwalsh@mail.pse.umass.edu

compatible solvents or fully incompatible non-solvents. The form of the proposed model predicts a critical dilatational stress at which the swelling is unbounded [3].

The intent of this study is to investigate whether the critical dilatational stress embodied in the Gent hypothesis can be observed by a change in the thermodynamic interaction between the liquid and polymer with respect to the hydrostatic stress state. The thermodynamic indicator chosen is the three phase contact angle of a sessile drop of the surface-active liquid on a polymer substrate. Figure 1 shows the sample geometry and the equilibrium balance of surface energies as described by Young's equation (Eq. 1). If the unbounded swelling transition can be observed as a change in contact angle the testing procedure would avoid the need to wait for the kinetics of the crazing event to occur to indicate susceptibility to ESC for a given liquid-polymer system.

To observe an equilibrium contact angle that accurately reflects the solid-liquid (γ_{SL}), solid–vapor (γ_{SV}), and liquid vapor (γ_{LV}) surface energies it is necessary to minimize the distortion of the sessile drop by gravitational forces and inertial forces. Useful quantitative criterion [7] are that the sessile drop diameter should be much smaller than the capillary length, $[\gamma_{LV}/\rho g]^{1/2}$, and the capillary velocity $[U_\mu/\gamma_{LV}]$) of the three phase line, should be much less than 10^{-4}.

$$\underbrace{\lim}_{\Delta A \to 0} \frac{\Delta G_s}{\Delta A} = 0 = \gamma_{SL} - \gamma_{SV} + \gamma_{LV} \cos\theta \qquad (1)$$

Typical ESC agent/polymer combinations have similar solubility parameters and thus low contact angles of approximately 15° or less. Conventional techniques of measuring contact angle using a microscope and goniometer have error in the range of ±2° to ±5° due largely to the subjective nature of choosing the tangent line at the sessile drop edge [8]. A precise and objective measurement method was needed that could be used

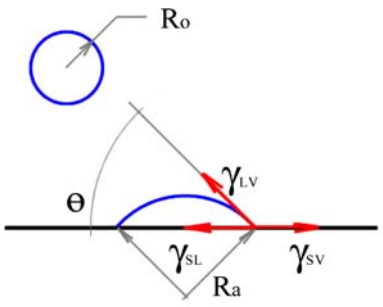

Fig. 1 Sample geometry showing sessile drop on substrate and balance of surface energies described by Young's equation

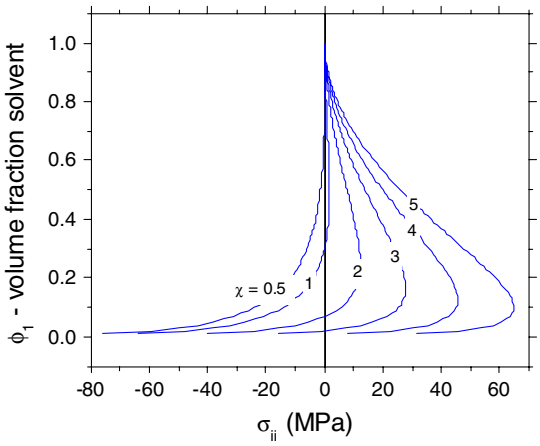

Fig. 2 Plot of Gent's generalization of the Flory–Huggins equilibrium swelling relationship for a physically cross-linked network showing solvent volume fraction versus hydrostatic stress for level curves of χ

in-situ during a tensile test experiment. The approach adopted was to use the refraction of a LASER through the lens of the sessile drop. This is a new method of measuring contact angle inspired by a method used by Langmuir and Schaeffer in which the angle of total specular reflection of a point source was measured at the sessile drop edge [9], and a remark by deGennes in his review of the statics and dynamics of surface wetting in which the reflection or deflection of light through the lens of the sessile drop is suggested as an appropriate method for very small contact angles [7]. A related technique involving reflection and refraction was also used by Rondelez et al. for measuring small contact angles [10].

Theoretical

Gent hypothesis of stress induced swelling

Gent's hypothesis proposes that there is a critical hydrostatic stress at which the polymer undergoes a glass to rubber transition as indicated by Eq. (2) [3]. If we consider the polymer as a physically entangled network then the equilibrium swelling of the network by a solvent can be described by the Flory–Huggins relationship [11]. This relation ship takes into account the entropy and enthalpy of mixing and the elastic strain energy and is described by the left hand side of Eq. (3) while the right hand side term describes the effect of the applied hydrostatic stress σ_{ii}. ϕ_2 is the volume fraction of polymer, χ is the polymer-solvent interaction parameter, V_1^m is the molar volume of the

solvent, ρ_2 is the polymer density and M_c is the molecular weight between cross-links.

$$\sigma_{ii}^{c} = \frac{(\phi_2 T_g - T)(\alpha_r - \alpha_g)}{C_r - C_g} \quad (2)$$

$$\ln(1-\phi_2) + \phi_2 + \chi\phi_2^2 + \frac{V_1^m \rho_2}{M_c}\left(\phi_2^{\frac{1}{3}} - \frac{\phi_2}{2}\right) = \frac{\sigma_{ii} V_1^m}{RT} \quad (3)$$

Figure 2 shows plots Gent's generalized Flory–Huggins relationship between hydrostatic stress and the volume fraction of solvent in a polymer for the cases of a compatible liquid with $\chi \leq 0.5$, and relatively incompatible liquids with $\chi > 0.5$ The level curve of $\chi = 0.5$ predicts that a compatible liquid (solvent) will swell the polymer rapidly with no applied positive hydrostatic stress. The level curves for $\chi > 2$ predict that the polymer will swell only slightly as hydrostatic stress increases until a critical stress level (σ_{ii}^{c}) is reached and at this critical level swelling becomes unbounded. As the incompatibility between the surface-active liquid and polymer, represented by χ increases, more hydrostatic tension is needed to allow swelling. For example: as χ increases from 2 to 3 σ_{ii}^{c} increases from ~15 MPa to ~30 MPa.

A valid criticism of Gent's hypothesis is that in the original derivation of the Flory–Huggins relationship assumptions were made that there are no preferential interactions between the solvent and solute and that the solvent molecule and polymer chain segment are of similar size. In the dilute solution regime contemplated by Flory–Huggins the disruption of entropy due to these preferential interactions is small enough that it is considered negligible however, this may not be true for a small molecule swelling a polymer network, and in the case of swelling a network the polymer chain segment is generally larger than the solvent species. Regarding the problem of size mismatch it should also be noted that Gent [12] and Treloar [13–15] both have used the same approach to successfully model equilibrium swelling of lightly cross-linked rubber networks by small homologous alkanes so the difference in size is probably less significant than the presence of specific interactions between the polymer solute and solvent species.

Experimental

Contact angle by refraction

The refraction technique is based upon the refraction of a laser beam through both a polymer substrate and lens of the sessile drop and the dry polymer substrate as shown in Fig. 3. The difference in refractive indices of the liquid and the surrounding vapor phase causes the transmitted light to diverge into two paths. The angles α, β, and the refractive indices of the gas (n_1), and the liquid (n_2), can be used to calculate the three phase contact angle (θ) according to Eq. (4).

$$\tan\theta = \frac{n_1(\sin\beta - \sin\alpha)}{n_2\left(1 - \left(\frac{n_1}{n_2}\right)^2 \sin^2\alpha\right)^{\frac{1}{2}} - n_1 \sin\beta} \quad (4)$$

The experimental device is shown schematically in Fig. 4. The substrate material is held in a horizontal fixture upon which a mechanical stress can be introduced with a mass or other mechanical testing system. Once a drop is applied, the transmitted light incident on the vertical detector is photographed using a CCD camera. The resulting images are used to determine the dimensions Z_α and Z_β. Subsequently, the angles α and β may be calculated from the X, Z_α and Z_β measurements. An

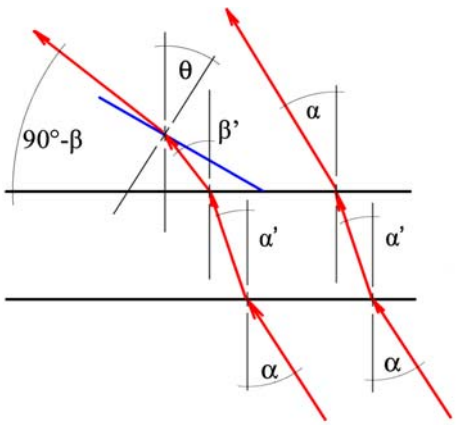

Fig. 3 Schematic of refraction geometry showing refraction of incident LASER through sessile drop lens and substrate material

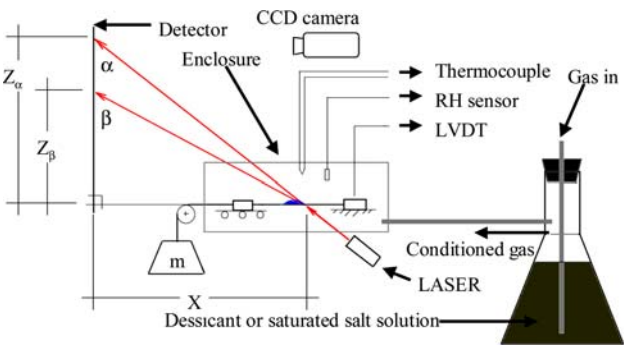

Fig. 4 Schematic of refraction device showing tensile sample, sessile drop, means of applying load, environmental enclosure, detector and LASER source

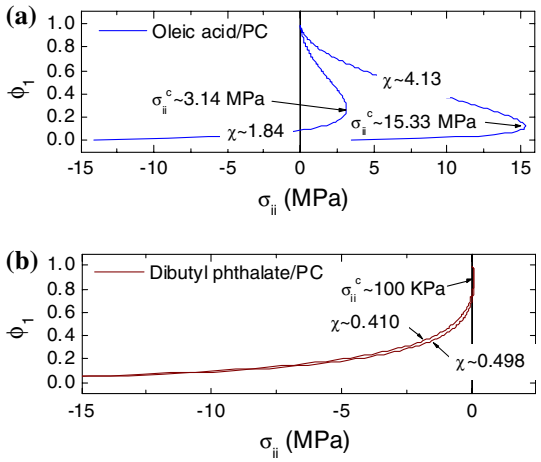

Fig. 5 Gent hypothesis prediction of critical hydrostatic stress for unbounded swelling for (**a**) oleic acid-polycarbonate and (**b**) dibutyl phthalate systems using χ as estimated from solubility parameter differences and the Hildebrand–Scatchard equation

enclosure around the sample ensures protection from airborne particles and gives the ability to control the nature of the vapor phase. An Schaevitz EC-250-DC LVDT is used to monitor the strain condition of the tensile bar, temperature is monitored using a K type thermocouple, and an Honeywell HIH 3610 relative humidity sensor is used to record the relative humidity of the vapor phase.

Materials

The substrate used was a 0.25 mm thick polycarbonate (PC) film purchased from McMaster Carr. M_n is ~11,000 g mol^{-1}, ρ is 1.2 g cm^{-3}, γ_{SV} is 42.9 mJ m^{-2} at 20 °C [16] and δ is in the range of 20–21 MPa$^{1/2}$ [17]. Polycarbonate samples were cut into standard ASTM 638 Type 1 tensile bars insuring that the machine direction was parallel with the direction of applied stress. The roughness of the PC substrate was characterized using a profilometer: perpendicular to the machine direction the arithmetic average roughness (R_a) was 44.8 nm and parallel to the machine direction R_a is 57.0 nm. The surface-active liquids, oleic acid and dibutyl phthalate, were chosen based on their solubility parameters relative to the PC substrate, comparable molecular weights, and low vapor pressures, which renders evaporation of liquid from the sessile drop negligible at standard conditions of temperature and pressure. Oleic acid is a monounsaturated lipid with MW of 282.47 g mol^{-1}, ρ is 0.8,634 g cm^{-3}, γ_{LV} at 20 °C is 33 mJ m^{-2} ±0.64 and δ is 15.6 MPa$^{1/2}$ [17]. It is not a solvent or strong swelling agent for PC. In contrast, dibutyl phthalate is a plasticizer with MW of 278.34 g mol^{-1}, ρ is 1.047 g cm^{-3}, γ_{LV} is 34 mJ m^{-2} at 20 °C and δ is 20.2 MPa$^{1/2}$ [17]. It can be expected to swell PC spontaneously.

The polymer-solvent interaction parameter χ can be estimated from the solubility parameters of the two materials using the Hildebrand–Scatchard relationship described in Eq. (5) where χ_s is an empirical parameter representing the entropic component of χ taken as approximately 0.35, and the term involving the difference in solubility parameters represents the enthalpic component of χ [17]. V_1^m is the molar volume of the solvent, δ_1 is the solubility parameter for the solvent, and δ_2 is the solubility parameter of the polymer.

$$\chi = \chi_s + \frac{V_1^m(\delta_1 - \delta_2)^2}{RT} \tag{5}$$

Figure 5(A) and (B) show the Gent hypothesis predictions of solvent uptake for the oleic acid-polycarbonate and dibutyl phthalate-polycarbonate systems. The predicted range of critical hydrostatic stress for oleic acid-polycarbonate is between 3.14 MPa and 15.33 MPa, and for dibutyl phthalate-polycarbonate is approximately 0–100 KPa.

Procedure

Contact angle, temperature, relative humidity, and strain were observed for five axially loaded tensile specimens for each of six discrete hydrostatic stress levels between 1 MPa and 13 MPa. The substrate surface was cleaned using a Chem-wipe lightly saturated with ethanol, then wiped dry with a fresh Chem-wipe and allowed to dry completely. The substrate film was clamped in the horizontal fixture, the LVDT set to the null position, and the LabView data collection system initated. At 30 s the mass was applied to the free end of the fixture resulting in a uniaxial stress on the substrate. After the load was applied a 1 μL sessile drop of oleic acid was applied to the middle of the gauge length using a micrometer syringe. This sequence is used to avoid affine deformation of the sessile drop. This volume resulted in a sessile drop of approximately 5 mm diameter, well below the capillary lengths for oleic acid and dibutyl phthahlate. The 0.10 mW, 640 nm Type II LASER source had been previously adjusted so that the incident beam was normal to the tangent edge of the sessile drop viewed from above. A CCD camera collected images of the refraction at intervals of 300 s beginning at the time of deposition. The X dimension was measured at 300 s and at 1,800 (oleic acid) or 3,600 (dibutyl phthalate) seconds. Typically ΔX was approximately 0.5–1 mm

Table 1 Estimate of maximum error (E_{max}) and uncertainty (U) in contact angle for oleic acid-polycarbonate system showing probable limiting precision of the refraction technique to be approximately 0.5°

θ	E_{max}	U
0°	±0.64°	±0.50°
1.31°	±0.65°	±0.50°
2.60°	±0.65°	±0.49°
3.88°	±0.65°	±0.49°
5.14°	±0.65°	±0.48°
6.37°	±0.65°	±0.47°
7.57°	±0.65°	±0.46°
8.73°	±0.64°	±0.45°
9.86°	±0.64°	±0.44°
10.94°	±0.63°	±0.43°
11.96°	±0.62°	±0.41°
12.93°	±0.60°	±0.40°
13.84°	±0.59°	±0.38°

during the duration of the experiment inferring a low average capillary velocity on the order of 10^{-7} for both surface-active agents. The time resolved refraction images were then analyzed using the UTHSCSA ImageTool ver. 3 software to determine Z_α and Z_β.

Results and discussion

Refraction images

Figure 6(A) is a CCD image of a representative refraction pattern for an PC substrate and sessile drop of oleic acid at a low uniaxial stress of approximately 3 MPa. The upper α refraction spot is light that has been refracted through the substrate only while the lower β refraction spot is light that has been refracted through both the substrate and the sessile drop edge. The irregularity of the β refraction spot is thought to be due to the serrated shape of the sessile drop-substrate interface and the resulting error in the Z_β measurand is the largest single source of error in this technique. Figure 6(B) is a dark field image of the sessile drop edge viewed from above using an optical microscope in reflectance mode. The dark regions are areas with low angle and the lighter region are areas with higher angle. The image shows that the triple line interface is not the idealized planar wedge embodied in Young's equation. This variation in contact angle near the triple line could be due to either roughness or chemical contamination of the substrate surface.

Using standard error propagation techniques [18], the maximum error E_{max}, and uncertainty U, can be estimated by Eqs. 6 and 7 where; R is the functional relationship between $\tan(\theta)$ and the experimental measurands X, Z_α and Z_β ; and P_X, and P_{Z_β} are the respective precisions of the measurands as estimated from a large body of refraction images for both oleic acid-polycarbonate and dibutyl phthalate-polycarbonate systems. Table 1 shows E_{max} and U for the range of angles accessible to this device assuming $P_X \approx \pm 2$ mm, $P_{Z_\alpha} \approx \pm 2$ mm and $P_{Z_\beta} \approx \pm 5$ mm. In general, the uncertainty U is considered to be a better estimate of probable error than E_{max} and the calculations show an expected uncertainty of the contact angle measurement to be approximately 0.5°. This is taken as the probable limiting precision of the refraction technique for these combinations of substrate material and sessile drop liquid.

$$E_{max} = \left|P_X \frac{\partial R}{\partial X}\right| + \left|P_{Z_\alpha} \frac{\partial R}{\partial Z_\alpha}\right| + \left|P_{Z_\beta} \frac{\partial R}{\partial Z_\beta}\right| \tag{6}$$

$$U = \left[\left(P_X \frac{\partial R}{\partial X}\right)^2 + \left(P_{Z_\alpha} \frac{\partial R}{\partial Z_\alpha}\right)^2 + \left(P_{Z_\beta} \frac{\partial R}{\partial Z_\beta}\right)^2\right]^{\frac{1}{2}} \tag{7}$$

The time resolved refraction images also allow the determination of the time at which craze damage is commensurate with the LASER wavelength λ occurs. This is accomplished by observation of the onset of diffraction fringes caused by the parallel array of closely spaced crazes. Figure 7 compares early and later time refraction images for an oleic acid-polycarbonate sample at a hydrostatic stress of ~13 Mpa. The

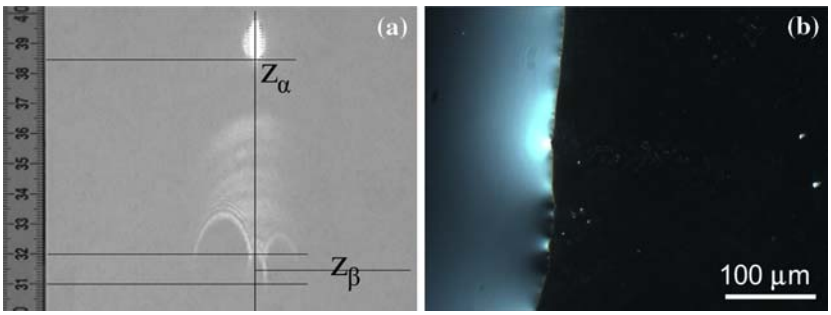

Fig. 6 (**a**) Oleic acid/polycarbonate refraction pattern showing measurands Z_α, and Z_β. (**b**) Reflectance mode optical micrograph of oleic acid/polycarbonate sessile drop edge viewed from above

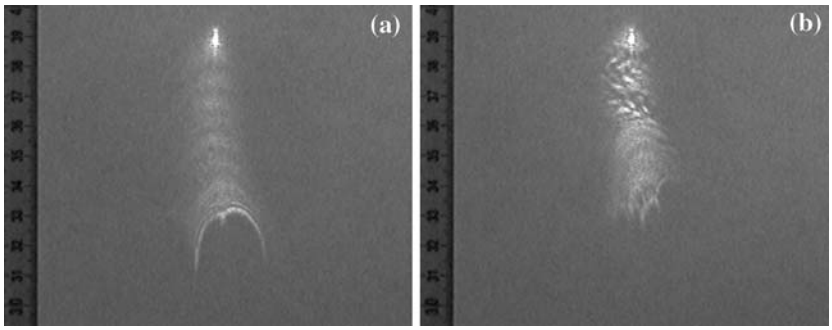

Fig. 7 Comparison of refraction images of an oleic acid-polycarbonate sample both prior to crazing (**a**), and after crazing (**b**). The diffraction fringes are used as indicators of crazes evolved to a size commensurate with the wavelength of the LASER source

early time image has no diffraction fringes while the later time image shows distinct diffraction fringes. The transition to diffraction fringes is observed before crazes in the tensile sample are easily visible to the naked eye and are believed to be associated with the craze pattern diffracting with the LASER.

Kinetics of craze initiation

It is generally recognized that craze initiation has a stress-time dependence and that the time at the onset of crazing decreases exponentially with increasing stress [1]. Using the diffraction fringes described in the previous section as an early indicator of craze formation, a time for craze initiation (t_c) was determined for increasing levels of stress. Figure 8 is a plot of the mean of repeated observations of t_c at three discrete hydrostatic stress levels for both the oleic acid-polycarbonate and dibutyl phthalate-polycarbonate systems. The error bars indicate a 95% confidence interval on the mean. The data confirm the previously observed exponential decrease in t_c with increasing stress. A first order exponential decay model was fitted to the data and is plotted as a dashed line along with the equilibrium values. In a kinetically limited process the infinite time equilibrium value will approach that of thermodynamic equilibrium. In these observations the $t \rightarrow \infty$ value of hydrostatic stress for crazing to occur is similar to the range of critical hydrostatic stress (σ_{ii}^{c}) values predicted by the Gent hypothesis for both surface-active liquids.

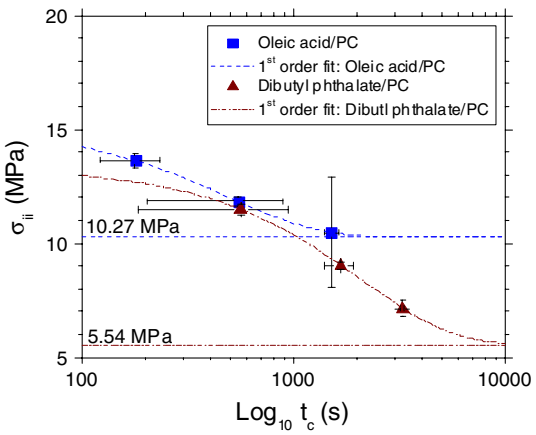

Fig. 8 Semilog plot of hydrostatic stress versus time to crazing for oleic acid-polycarbonate and dibutyl phthalate-polycarbonate systems showing that t_c decreases with increasing stress for both cases, and that the value of stress at which crazing occurs given infinite time is similar to the critical hydrostatic stress predicted by the Gent hypothesis

However, some limitations of this data set need consideration: the experimental duration of one hour is short and so crazing was not often observed under conditions of lower stress; also, the effect of viscoelastic creep of the loaded tensile sample, and the fraction of the test section surface area affected by the surface-active liquid may have effects on t_c that are difficult to deconvolute. Longer observation times at lower stress in which there is little or no creep, and test geometries in which the surface-active liquid is in contact with the entire test section would enable a more reliable statistical distribution of t_c with respect to stress and yield a more meaningful equilibrium value of σ_{ii}^{c}.

Strain condition at crazing

The strain at the onset of crazing as determined by the development of diffraction fringes in the refraction image was observed. Figure 9 shows plots of hydrostatic stress versus the total strain at crazing and hydrostatic stress versus the inelastic strain at crazing for both surface-active liquids.

The strain at crazing can generally be said to increase with stress for both systems. The dibutyl phthalate-polycarbonate crazes at lower levels of stress than the oleic acid-polycarbonate system and shows an approximately linear relationship between hydrostatic stress and crazing strain. The oleic acid-polycarbonate system has quite a bit of scatter and no linear relationship can be inferred. In the oleic acid-polycarbonate

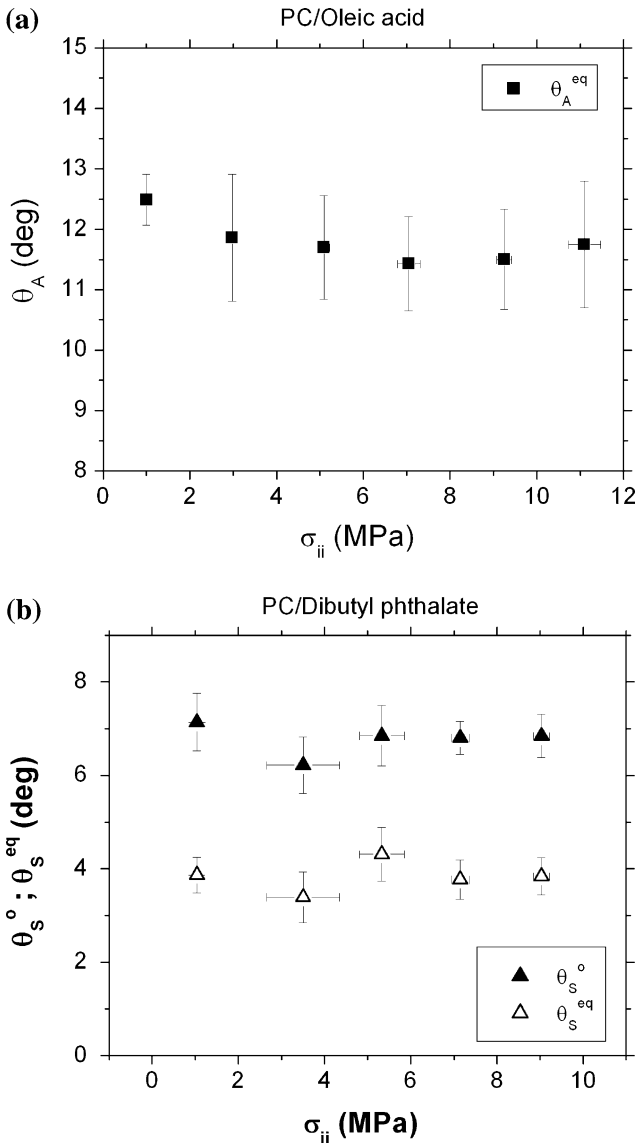

Fig. 9 Plots of total strain at crazing and inelastic strain versus hydrostatic stress for (**a**) oleic acid-polycarbonate and (**b**) dibutyl phthalate-polycarbonate systems

observations the lowest level of stress at which crazing occurred during the duration of the experiments was ~11–12 Mpa—this is within the range of critical hydrostatic stress predicted by the Gent hypothesis.

Comparison of the inelastic strain at crazing data shows markedly different behavior between the two surface-active liquids. The dibutyl phthalate-polycarbonate system crazes at essentially zero inelastic strain at all stress levels tested larger than zero. The oleic acid-polycarbonate system shows two distinct regions of inelastic strain response. At hydrostatic stress below 11–12 MPa the inelastic strain at crazing is highly variable between 0.1–0.6%. At stress levels above 12 MPa the inelastic strain at crazing is less than 0.1%. This transition in behavior occurs near the midpoint of the range of hydrostatic stress predicted by the Gent hypothesis and could be taken as evidence of increased swelling at larger stress.

Kambour [1], and Arnold [19] have respectively proposed critical strain criterion, and critical inelastic strain criterion for crazing. It should be noted that any attempt to correlate a critical strain or inelastic strain using this data is complicated by the fact that the surface-active agent is in contact with only a small area of the gauge length of the tensile specimen. In this experimental geometry the strain response to stress is a composite of the dry polymer response and that of the region affected by the surface-active liquid.

Contact angle observations

Figure 10 shows a comparison of the advancing contact angle versus time for the oleic acid-polycarbonate and dibutyl phthalate-polycarbonate systems at a low level of hydrostatic stress. The data represent the mean of five samples under identical conditions and the error bars are a 95% confidence interval on the mean. The

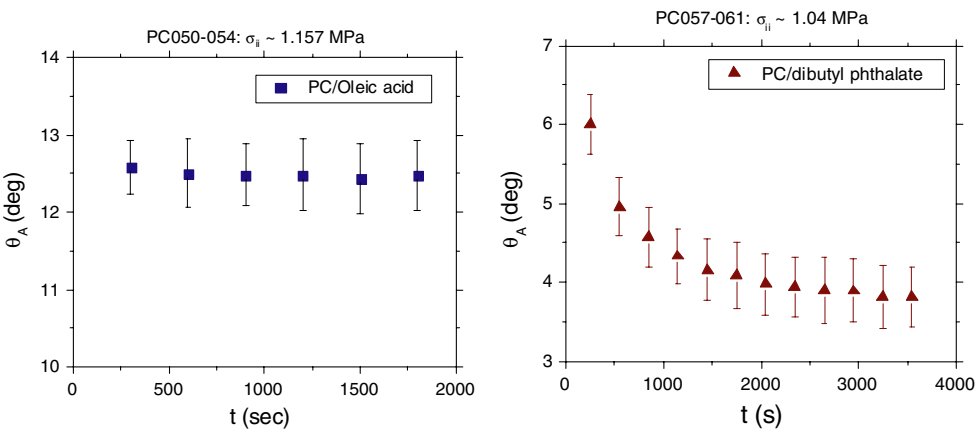

Fig. 10 A comparison of advancing contact angle versus time for oleic acid-polycarbonate and dibutyl phthalate systems at low hydrostatic stress

oleic acid has a larger solubility parameter mismatch with PC than the dibutyl phthalate and shows no significant decay of contact angle with time. The dibutyl phthalate has nearly the same solubility as PC and shows strong decay with time. This indicates that if swelling occurs contact angle is a sensitive metric of absorption of the liquid into the substrate. The rate of decay observed in the dibutyl phthalate-polycarbonate system did not change significantly with increasing stress.

Figure 11(A) shows a plot of advancing contact angle versus stress for the oleic acid-polycarbonate system under increasing levels of hydrostatic stress. The data points are the mean of five samples each observed for 1,800 s and the error bars for angle and hydrostatic stress are the 95% confidence interval. No transition of contact angle with hydrostatic stress is evident. The error bars indicate that the precision achieved was ±1° a value greater than the limiting precision of 0.5° suggested by the previously described error analysis and achieved in other observations. Subsequent experiments probing the effect of relative humidity on contact angle are reported in Fig. 12 and show a strong influence. The increased variation may be due to variation in relative humidity in the sample environment for this set of experiments.

The dibutyl phthalate-polycarbonate samples show decay in contact angle with time—both the initial and equilibrium contact angles as determined by first order exponential fits are reported in Fig. 11(B). The data points are the mean of five samples each observed for 3,600 s and the error bars for angle and hydrostatic stress are the 95% confidence interval. Again, there was no significant transition of contact angle with hydrostatic stress for either initial or equilibrium contact angle.

The data for higher levels of stress indicate that even after crazing occurred in a sample, and the surface topography altered by crazing, the effect on the advancing contact angle was not significant. Although both the kinetics of craze initiation and the inelastic strain condition at crazing imply the existence of a transition near Gent's critical hydrostatic stress, the three phase advancing contact angle does not indicate any such transition.

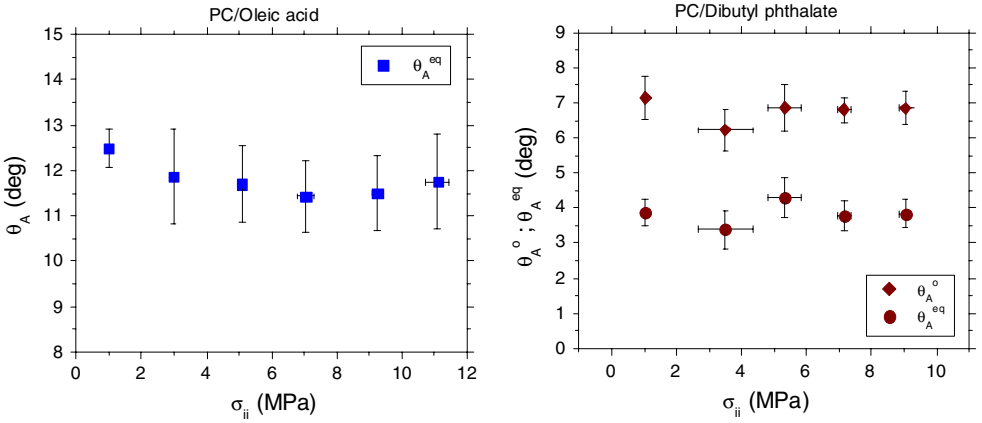

Fig. 11 (**a**) Plot of advancing contact angle versus hydrostatic stress for oleic acid-polycarbonate, (**b**) plot of initial and equilibrium advancing contact angles versus hydrostatic stress for dibutyl phthalate-polycarbonate

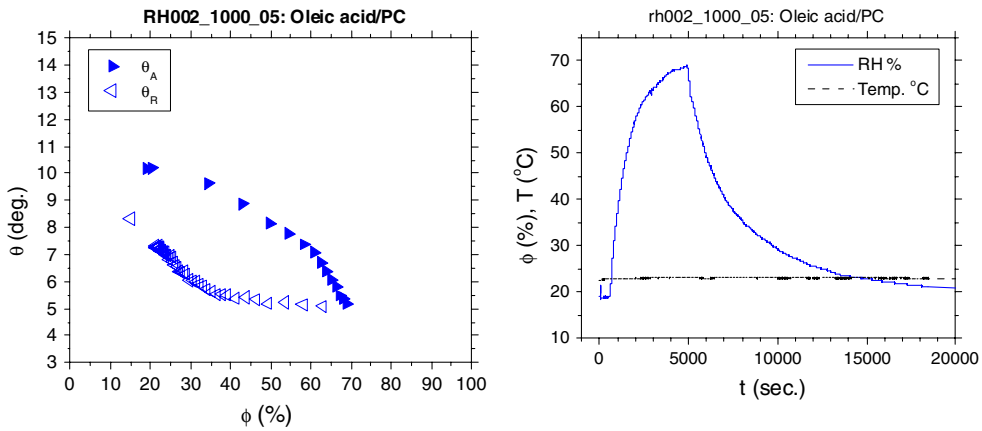

Fig. 12 Plot of contact angle (θ) versus relative humidity (ϕ) for oleic acid-polycarbonate system at low stress showing significant hysteresis between advancing and receding angles

Figure 12 shows contact angle observations for an oleic acid-polycarbonate system under changing conditions of relative humidity (ω). The humidity conditions as shown in the inset graph of ω versus time begin at 20% are cycled up to 70% then cycled down from 70% back to 20%. As relative humidity is increased the contact area of the sessile drop spreads and the contact angle drops. The triple line is translating onto dry substrate so the contact angle data are advancing angles (θ_A). As the relative humidity is decreased back from 70% the contact area is at first pinned then retracts. The triple line is receding from wetted substrate and the contact data are receding angles (θ_R). Each observation of contact angle was taken at a 300-second interval and so the plot shows that the contact area of the sessile drop spreads onto dry substrate more readily than it recedes.

The large degree of hysteresis between the advancing and receding angles, and the pinning evident in this data, illuminates a drawback in using contact angle to monitor transitions in γ_{SL}. For the oleic acid-polycarbonate system the magnitude of contact angle hysteresis is on the order of 3°–5°. Contact angles within the limits of θ_A and θ_R are in thermodynamic equilibrium, and the effect of changes in γ_{SL} on θ could reasonably be expected to be smaller than this given the localized nature of the swelling proposed in the Gent hypothesis. In this light, any changes in θ related to Gent's transition to unbounded swelling could easily be obscured by pinning of the sessile drop between the limits of the advancing and receding angles.

The hysteresis between advancing and receding angles can be considered as an indicator of the work of adhesion between the liquid and substrate. Future experiments are planned that will look at the magnitude contact angle hysteresis as a function of stress to see if Gent's transition to unbounded swelling is indicated.

Conclusions

The refraction technique has proven to be an objective and precise method of measuring sessile drop contact angles of less than 15°. The precision of ±0.5° is an improvement on the 2°–5° precision of conventional goniometer/microscope methods and approaches the ±0.1° precision of axis-symmetric drop shape analysis (ADSA) methods. Limitations of the refraction technique are that both substrate and liquid must be optically clear, and the environment of the sessile drop must be carefully controlled for temperature, humidity and airborne contaminants.

No transition in contact angle as a function of hydrostatic stress was observed in either the oleic acid-polycarbonate or the dibutyl phthalate-polycarbonate experiments. If, as proposed by Gent, a transition is actually occurring at localized areas of stress concentration the large hysteresis between advancing and receding angles may obscure it because the expected changes in solid-liquid surface energy are too small to overcome the pinning of the triple line at some angle intermediate to the advancing and receding angles. Nevertheless, these observations of contact angle with respect to polymer stress state do not support the thermodynamic transition implied in the Gent hypothesis

The kinetic observations of hydrostatic stress and time to crazing were conducted on a very short time scale and so are of limited value in drawing quantitative conclusions, but the long time hydrostatic stress at crazing determined from a fit of the data is in the same range as the critical hydrostatic stress predicted by the Gent hypothesis. Similarly the hydrostatic stress and inelastic strain at crazing qualitatively imply a transition near Gent's critical hydrostatic stress.

The observations of the effect of changing vapor phase on the sessile drop contact angle point to a simple method of measuring contact angle hysteresis. Future experiments are planned to look at the effect of stress state on the magnitude of hysteresis for ESC liquid/polymer combinations.

Acknowledgements We would like to acknowledge the generous support given this work by the Materials Research Science & Engineering Center on Polymers at the University of Massachusetts (MRSEC) and Cluster M of the Center for University of Massachusetts-Industry Research in Polymers (CUMIRP). Cluster M member companies include: Atofina, Essilor USA, Henckel Loctite, International Paper and Meadewestvaco.

References

1. Kambour RP (1973) Macromol Rev 7:1
2. Raman A, Farris RJ, Lesser AJ (2003) J App Polymer Sci 88:550
3. Gent AN (1970) J Mater Sci 5:925
4. Mai YW (1986) J Mater Sci 21:904
5. Yee AF (2000) Macromolecules 33:1338
6. McGrath JE Parvatareddy H, Dillard JG, Dillard DA (1999) J Adhesion 69:83
7. de Gennes PG (1985) Rev Mod Physics 57:827
8. Kwok DY, Neumann AW (1999) In: Surface characterization methods; surfactant science series, vol. 87. Marcel Dekker, New York, NY, p 37
9. Langmuir I (1937) J Amer Chem Soc 59:2400
10. Rondelez F, Allain C, Ausserre D (1985) J Colloid Interface Sci 107:5

11. Flory PJ (1953) In: Principles of polymer chemistry. Cornell University Press, Ithaca, NY, p 576
12. Gent AN (1989) J Polaymer Sci Part B 27:893
13. Treloar LRG (1950) Trans Faraday Soc 46:783
14. Treloar LRG (1972) Polymer 13:195
15. Treloar LRG (1972) Polymer 13:203
16. Mark JE (1999) Polymer data handbook Oxford Univ. Press New York, NY p 363
17. Barton AFM (1983) In: CRC handbook of solubility parameters and other cohesion parameters. CRC Press, Boca Raton, FL
18. Mandel J (1964) In: The statistical analysis of experimental data. John Wiley & Sons, New York, NY, p 72
19. Arnold JC (1995) J Mater Sci 30:655